J. Fluid Mech. (1983), *vol.* 131, *pp.* 73–89
Printed in Great Britain

A closed-loop gravity-driven water channel for density-stratified shear flows

By D. C. STILLINGER, M. J. HEAD†, K. N. HELLAND, AND C. W. VAN ATTA†

Institute for Pure and Applied Physical Sciences and Department of Applied Mechanics and Engineering Sciences, University of California, San Diego, La Jolla, CA 92093

A closed-loop multilayer salt-stratified water channel allowing independent adjustment of velocity and density profiles has been developed for the study of stably stratified shear flows. Each of ten gravity-driven layers are adjustable for velocities from 0 to 30 cm/s and densities from 1.0 to 1.1 g/cm^3. A turbulence-management section located at the inlet manifold successfully suppresses undesired turbulence due to the ten mixing layers generated at this inlet. This management section also smooths the inherent step structure of the initial velocity and density profiles. Velocity profiles can be maintained throughout an experiment, whereas density profiles change slowly in time. An inner core region of linear stable density gradient will remain stationary for a time dependent on the initial stratification, velocity profile and mixing conditions. Temperature is observed to increase at a rate near 1 °C per hour due to internal heating in the system. A description of calibration techniques and temperature-correction methods for the velocity and conductivity instrumentation is described.

1. Introduction

Recent efforts to understand mixing processes in the ocean and atmosphere have emphasized the need to study the fundamental structure of turbulence under the influence of stratified density fields (Osborn 1980; Gibson 1980). However, it has been extremely difficult to obtain sufficiently comprehensive field measurements of the inherently small-scale statistical information necessary to investigate this motion (Gibson 1981). It is thus highly desirable to create simple turbulent stratified flows in the laboratory where the most basic interactions between buoyancy, inertial, and viscous forces can be investigated.

Grid turbulence, whose structure and behaviour is well known in the non-stratified case, is a useful first problem for studying dynamic differences due to buoyancy effects. Grid-generated turbulence has previously been produced in stratified fluids in two ways. Webster (1964), Lin & Binder (1967), Scotti (1969) and Montgomery (1974) used existing wind tunnels and differentially heated the fluid to stratify the flow field thermally. Others like Pao (1973), Lin & Veenhuizen (1974), Lange (1974) and Dickey & Mellor (1980) towed grids through large tanks of salt-stratified water. Here, we describe an alternative approach first employed by Stillinger (1981).

Odell & Kovasnay (1971) point out the limitations imposed by these facilities. Heated wind tunnels cannot attain strong density stratification without severely reducing the mean-flow values. The tunnel walls also must be carefully insulated or sources and sinks exist for temperature fluxes into the boundaries. Towing tanks on

† Also Scripps Institution of Oceanography.

the other hand use salt as the stratifying agent. Very precise experiments can be performed, but only short samples of steady-state conditions are possible. Repeatability of specific experimental conditions necessary to obtain statistically significant quantities of data becomes difficult. Data probes also must be towed behind the grid without inducing spurious motions, thus requiring high-precision tow methods. In response to these difficulties, they suggest a technique to establish a stable density gradient using salt in a closed-loop water channel. Unfortunately in their design they were able to maintain a distinct density profile only at very slow speeds, thus making it difficult to generate high-intensity turbulence.

This paper describes a new closed-loop water channel facility capable of generating arbitrary density and velocity profiles at the test-section inlet with sufficiently high mean speeds so that energetic turbulent flows can be generated in a variety of stratified configurations. The companion paper (Stillinger, Helland & Van Atta 1983) describes the influence of stable stratification on the behaviour of grid-generated turbulence in this facility.

2. Description of the apparatus

The stratified water-channel facility is shown in figure 1. A schematic block diagram of its major features is shown in figure 2. The system consists of a test section, ten pairs of reservoir tanks, inlet and outlet manifolds, and feed and return piping. The system is constructed of plastic to avoid corrosion. The clear test section is $30 \times 40 \times 500$ cm long wetted, with a 75 cm long entrance section containing turbulence-management devices. The test-section volume comprises about 10% of the total system capacity of 1600 gallons.

In operation water and salt are premixed to a suitable initial density in the lower reservoir tanks. Ten 1-horsepower centrifugal pumps lift the water to upper reservoir tanks, which are maintained at a constant level by overflow pipes. The overflow lines are able to handle the full flow rate of the pumps so that there is no lower limit on the speed achievable in the test section.

The upper tanks are baffled to force the flow path to make several vertical excursions within the tank. Most bubbles, which cause extreme difficulty when using hot-film anemometers, are thus removed. The baffles also tend to low-pass filter the disturbances induced by the inlet line running at constant maximum flow rate. There is little variation in head height in the last compartment and thus the delivery pressure to the channel is effectively constant.

Water is supplied to the test section through ten 3 in. diameter plastic pipelines. A Venturi tube and manometer on each line are used to monitor the flow rates. Since ten flow-measuring devices are necessary, this simple system was chosen over more costly methods. They provide a reliable and inexpensive flowmeter that only needs to be calibrated once. This calibration is also independent of the density of the water run through the Venturi tube as long as the manometer contains water of the same density. Valves are provided allowing the manometers to be flushed to the correct density of each tank before a run. The flow rates in each layer are set using multiturn brass gate valves.

The ten supply lines are joined to the test section by a transition section which connects the circular pipes to the rectangular inlet manifold while expanding uniformly to twice the pipe area. The ten layers are kept separate in the inlet manifold by splitter plates which end at the entrance to the turbulence-management section. This section consists of two sets of screens backed by an open-pore acoustic foam.

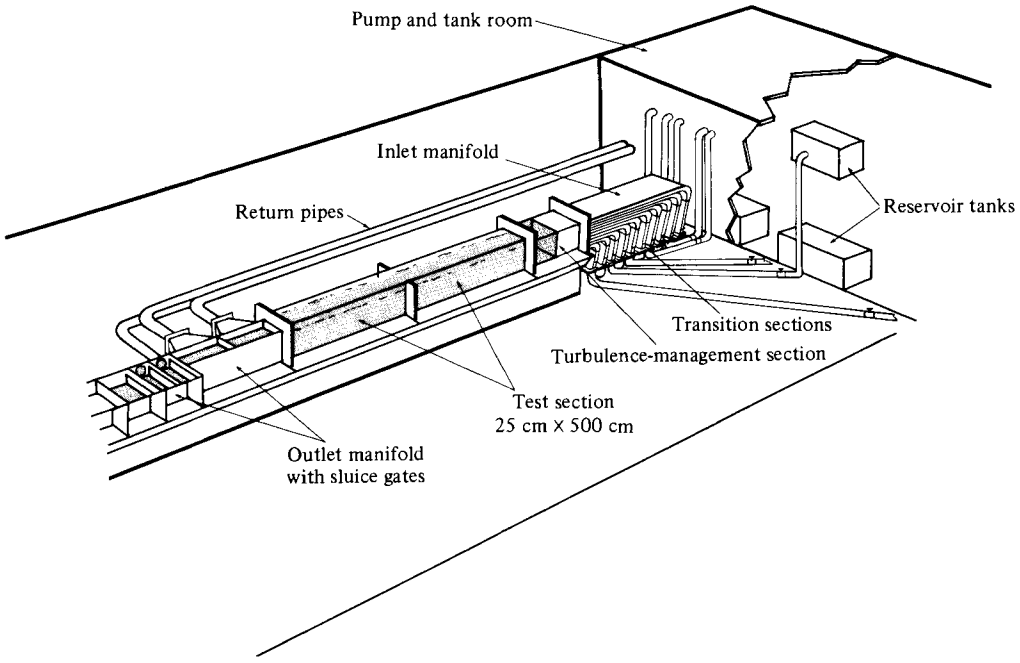

FIGURE 1. Perspective sketch of water-tunnel system.

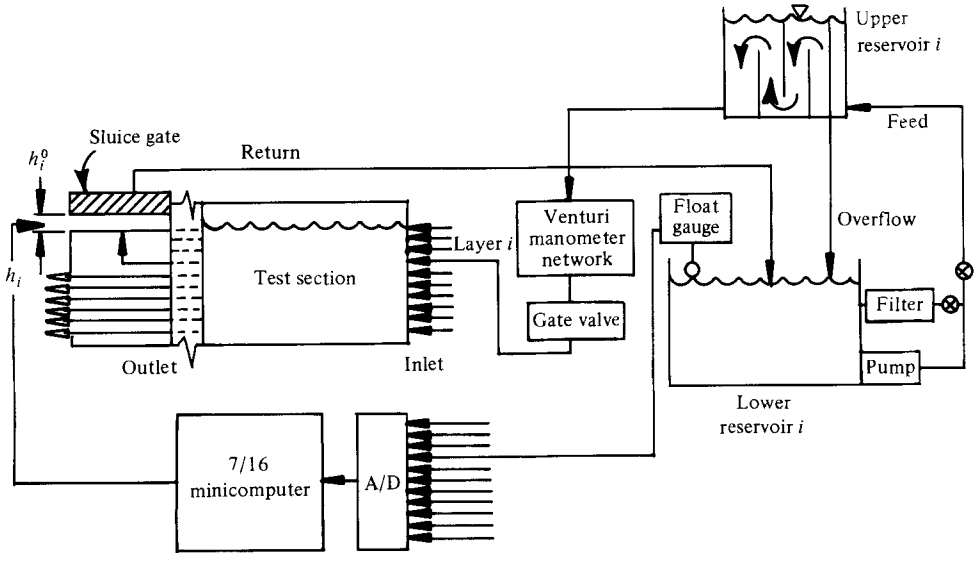

FIGURE 2. Schematic block diagram of water channel.

Together they reduce the background turbulence level and smooth out the discrete jumps in both the velocity and density profiles.

The test section is followed by the outlet manifold, which consists of another set of splitter plates and individual sluice gates for each layer. The splitter plates separate

the outgoing flow to reduce the mixing beyond that which takes place in the test section.

Sluice gates are used at the test-section outlet to provide a practical means of operating a multilayer channel with a free surface. They allow the test section to be full in the stationary condition and avoid complicated start-up procedures that other configurations might require. The adjustable sluice gates are nominally all at the same height and are designed to provide the proper back pressure on the flow in the test section. The sluice gates are adjustable in order to satisfy the very important constraint that the volumetric flow rate into the test section from each layer match the flow rate out of the test section in that same layer. If this matching condition is not invoked, there will be a gain or loss of water in some or all of the lower reservoir tanks.

The water is returned by gravity to the lower reservoir tanks by individual 4 in. pipelines. Each lower reservoir also has a 5 μm filter that can be switched into the pump circuit so that water can be circulated in the lower tanks before any run to mix the salt solutions and clean the water.

3. Velocity control

The maximum mean velocity of any layer is 30 cm/s. Any desired mean inlet velocity profile can be achieved by setting the ten gate valves. The outflows must be set by adjusting the sluice gates such that the flow rates match layer by layer.

The flow-rate matching is accomplished with an Interdata 7/16 mini-computer and ten float gauges. The float gauges give an electrical indication of the water level in each tank. By taking several samples spaced 30 seconds apart, the minicomputer calculates the rate of change of the water level for each tank. From this information the minicomputer calculates the corrections required for each sluice gate. The desired steady state is achieved when all 10 levels no longer change with time.

The procedure to predict the sluice-gate adjustment correction Δh for steady-state operation is based on a Taylor-series expansion of ten continuity equations in terms of sluice-gate height. Measured influence coefficients for each sluice gate are used to predict the correct height for all ten sluice gates. Let Q_i be defined as the difference between the inlet flow rate and outlet flow rate in layer i. This net flow rate can be considered as resulting from an error in the sluice-gate settings for all layers. Q_i then is a function of all ten sluice-gate openings, i.e.

$$Q_i = f_i(h_1^0, h_2^0, h_3^0, \ldots, h_{10}^0),$$

where h_j^0 is the height of sluice gate j relative to some common datum.

Define $\Delta h_j = h_j - h_j^0$, where h_j is a new height setting of gate j, then the Taylor series expansion of Q_1 is

$$Q_1(h_1, \ldots, h_{10}) = Q_1(h_1^0, \ldots, h_{10}) + \sum_{j=1}^{10} \frac{\partial Q_1(h_1^0, \ldots, h_{10}^0)}{\partial h_j} \Delta h_j + \ldots . \tag{1}$$

Higher-order terms are neglected. Equation (1) can be written in matrix form as

$$\boldsymbol{Q} = \boldsymbol{Q}^0 + \boldsymbol{Q}' \Delta \boldsymbol{h}, \tag{2}$$

where $\boldsymbol{Q}$ is the error flow-rate matrix for all sluice gates set to height h_j [10×1], $\boldsymbol{Q}^0$ is the error flow-rate matrix for all sluice gates set at initial height h_j^0 [10×1], $\boldsymbol{Q}'$ is the matrix of influence coefficients [10×10], and $\Delta \boldsymbol{h}$ is the height-change matrix [10×1].

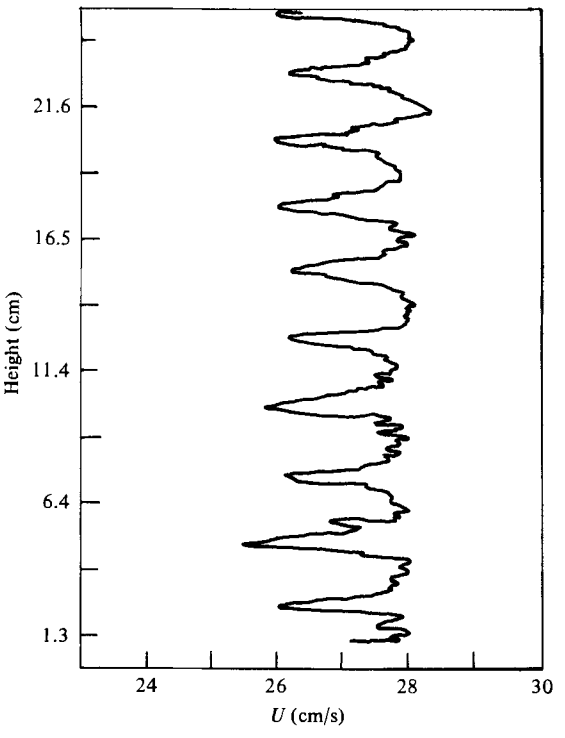

FIGURE 3. Velocity profile observed 0.5 cm downstream of the inlet manifold with turbulence-suppression apparatus removed.

The matrix $\boldsymbol{Q}$ is set equal to zero to find the height settings for steady state conditions, i.e.

$$\Delta \boldsymbol{h} = -\boldsymbol{Q}'^{-1}\boldsymbol{Q}^0. \tag{3}$$

$\boldsymbol{Q}'$ is determined during a pre-experiment fresh-water test. The experimental inlet velocity profile is established and a newer steady-state setting of the sluice gates is found by trial and error. Once this state is established $\boldsymbol{Q}'$ is measured by perturbing each sluice gate, one at a time, a given amount and observing the ten error flow rates that result. This is a complicated and time-consuming process, but needs to be done only once per velocity-profile type.

In operation the inlet profile is first adjusted using the manometers. Float-gauge readings are sampled at known time intervals and stored in the computer. Error flow rates are then calculated for each layer and (3) is used to generate a predicted height for each sluice gate that will bring the flow into a steady state. The method is convergent as long as the initial conditions are not too far from equilibrium. Experience has shown that two or three iterations will bring all the error flow rates below 0.5 gallons/min. Typical experiments routinely achieve error flow rates below 0.1 gallons/min.

4. Turbulence-management section

The turbulence-management section has two functions. It must suppress the background turbulence levels at the channel inlet and also smooth the discrete jumps present in both the density and velocity profiles. Without any turbulence-suppression

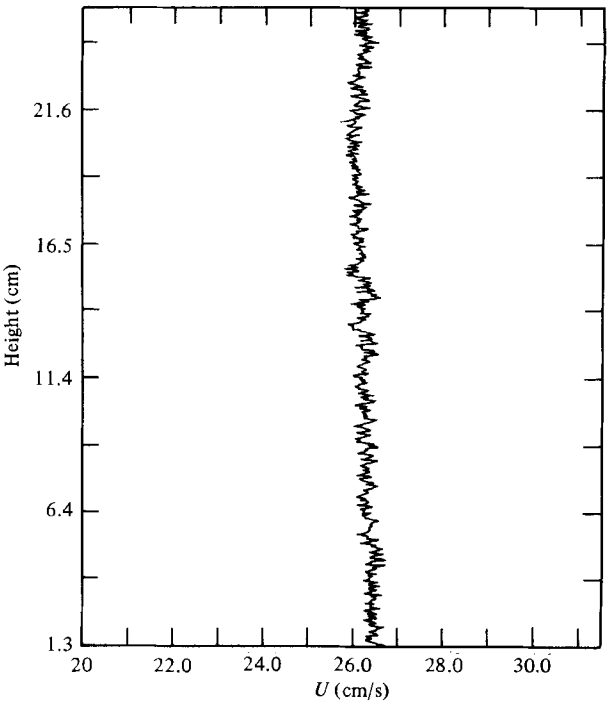

FIGURE 4. Velocity profile at the test-section inlet with turbulence-management section in place.

apparatus the inlet manifold produces ten 2-dimensional jets as shown in figure 3. These jets cause large-scale mixing due to the shear layers and introduce artificial lengthscales ordinarily not desired. In order to reduce this disturbance two screens (6 mm mesh) spaced 28 cm apart and each backed by 2.5 cm thick acoustic foam are placed in the channel. The first grid-and-foam combination is placed directly against the inlet splitter plates. This first suppressor breaks down the 2-dimensional jet structure and creates much smaller turbulent scales.

The mean profiles have lost most of their step structure as the flow approaches the second grid-and-foam combination. This grid–foam combination further reduces any large-scale motion remaining in the flow. Residual disturbances then decay until the test section is reached 47 cm downstream. A representative velocity profile monitored at the test-section entrance with the turbulent management section in place is shown in figure 4. The discrete nature of the profile has been effectively removed, and a smooth continuous gradient is produced. In all subsequent experiments ten data points measured on equally spaced intervals in the vertical were considered sufficient for monitoring the vertical gradients. Typical uniform and shear flows that can be produced are shown in figure 5. Mean-density profiles are similarly smoothed as shown in figures 8 and 10.

Figure 6 shows the effectiveness of the turbulence management section. Velocity measurements of the turbulent intensity level $(\overline{u^2})^{\frac{1}{2}}/\overline{U}$ were taken at stations downstream from a square-mesh biplane grid with rod diameter of 0.318 cm spaced 1.9 cm apart, placed at the test-section entrance with and without the management section in place. A non-stratified uniform velocity flow was used in this test. Without the management section the 2-dimensional jets produced large-scale motions that

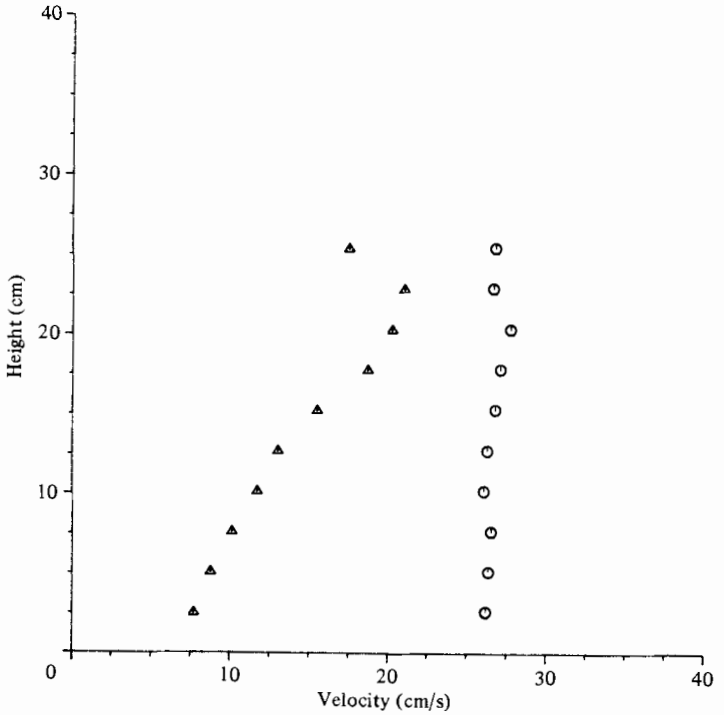

FIGURE 5. Typical velocity-profile configurations possible at the test-section inlet.

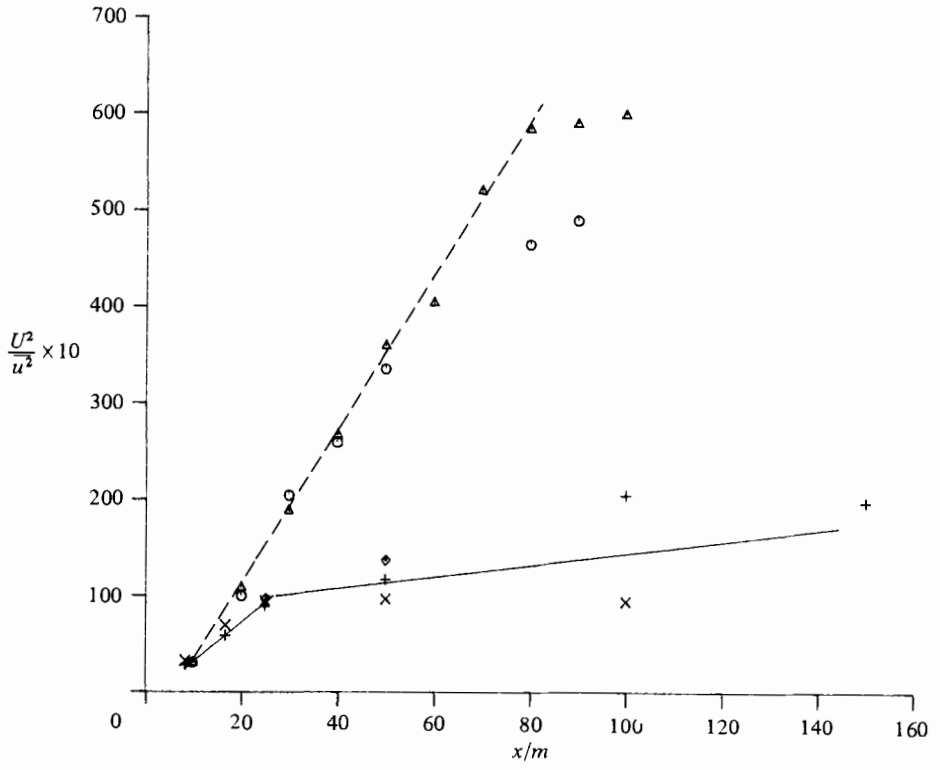

FIGURE 6. Decay of grid-generated turbulence in the test section under non-stratified flow conditions: ——, without turbulence-management section in place; ----, with turbulence-management section.

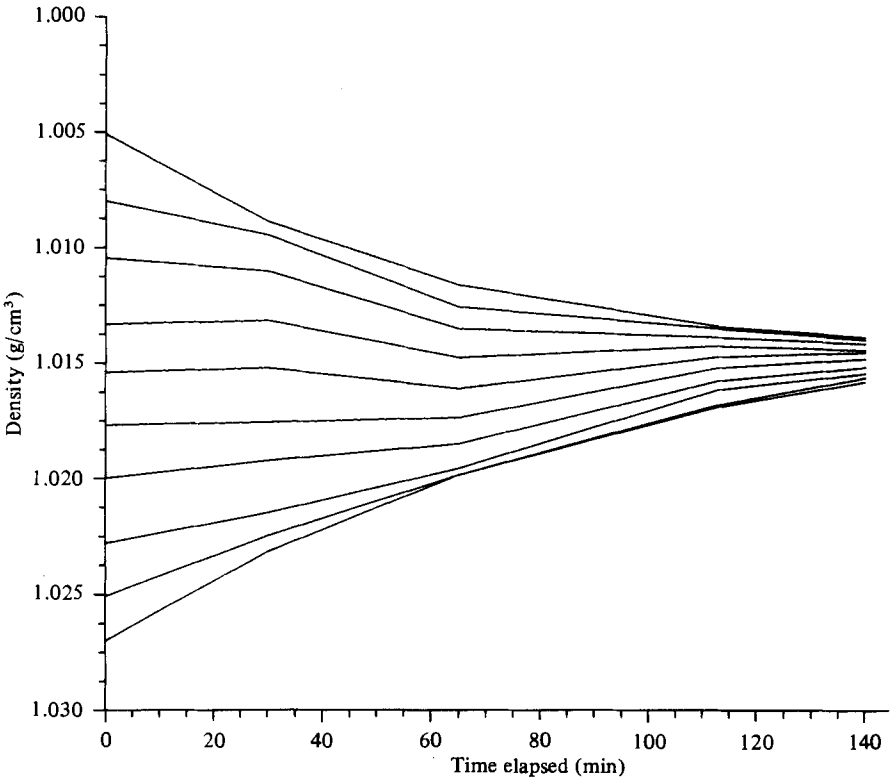

FIGURE 7. Density-profile decay for a uniform velocity profile with $\overline{U} = 25$ cm/s.

persisted the entire length of the test section. Turbulence-intensity levels decayed only up to $x/m = 30$ and then persisted at a background level of about 3.5%. The same figure shows that intensity levels were lowered to about 1.5% when the turbulence-suppression devices were utilized. Decay behind the grid continued until $x/m = 100$.

One drawback in using the turbulence-management section in a stratified flow field is that internal waves are generated. However, the high shears and larger scales present without the management section probably produce more waves on the interfaces of high density difference. The present suppression technique is the best compromise found for the geometry and flow conditions of the present channel design.

The management approach presented thus far works well for experiments having a uniform mean-velocity profile. If a sheared profile is desired, only the first screen-and-foam combination can be used because the second manager produces a large back pressure on the upstream flow. This results in the readjusting of the shear profile into one that is more uniform.

5. Density control

Any desired density profile is initially established by mixing appropriate amounts of salt and filtered deionized water in the ten lower reservoir tanks. Since water of different density is delivered to each layer, discrete jumps occur in the profile at the inlet manifold. As discussed in §4, the jumps are smoothed by the turbulence-

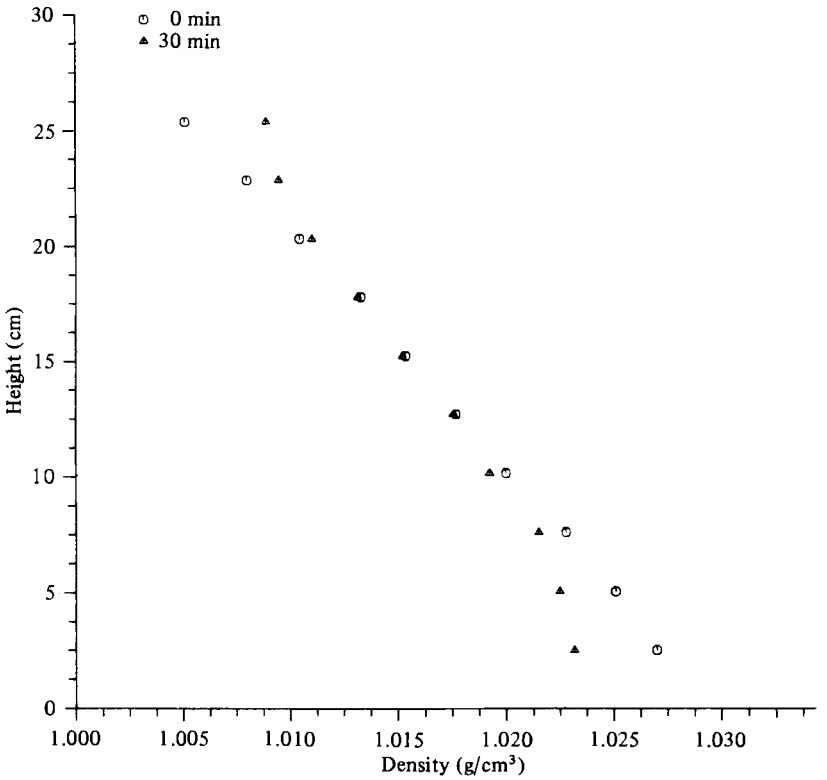

FIGURE 8. Density profiles at two times in a stratified experiment. Uniform velocity profile with $\overline{U} = 25$ cm/s.

management section and the desired mean-density gradient is generated. Two typical profiles are shown in figures 8 and 10.

A given density profile can be maintained for only a limited time at the test-section inlet. Mixing will occur in the test section, and water returned to the lower reservoirs will alter the fluid density in each tank. The decay of stable density profiles in the presence of uniform and shear velocity profiles are shown in figures 7 and 9. Both experiments illustrated used a biplane rod grid inserted at the front of the test section for the turbulence-decay studies.

Figure 7 shows that, with a uniform velocity profile, an inner core of the flow through the test section maintains a slowly changing density gradient for some time, while the boundary layers erode the top and bottom sections of the profile relatively quickly. Eventually, mixing due to turbulence from the grids, foam and the instrument sensor arrays cause the density profile to approach the fully mixed condition.

When a velocity shear is applied in the same experiment, the density gradient decays somewhat differently, as shown in figure 9. The low velocities at the channel bottom result in very little mixing of the profile there. The upper layers mix as in the uniform-velocity case. The central region again maintains a nearly constant gradient, but its decay is much slower. Less mixing occurs despite the presence of the shear because mean velocities are smaller in the central region resulting in lower turbulence intensities being produced by the grid. Production of turbulence from the mean-velocity gradient never makes up this deficit.

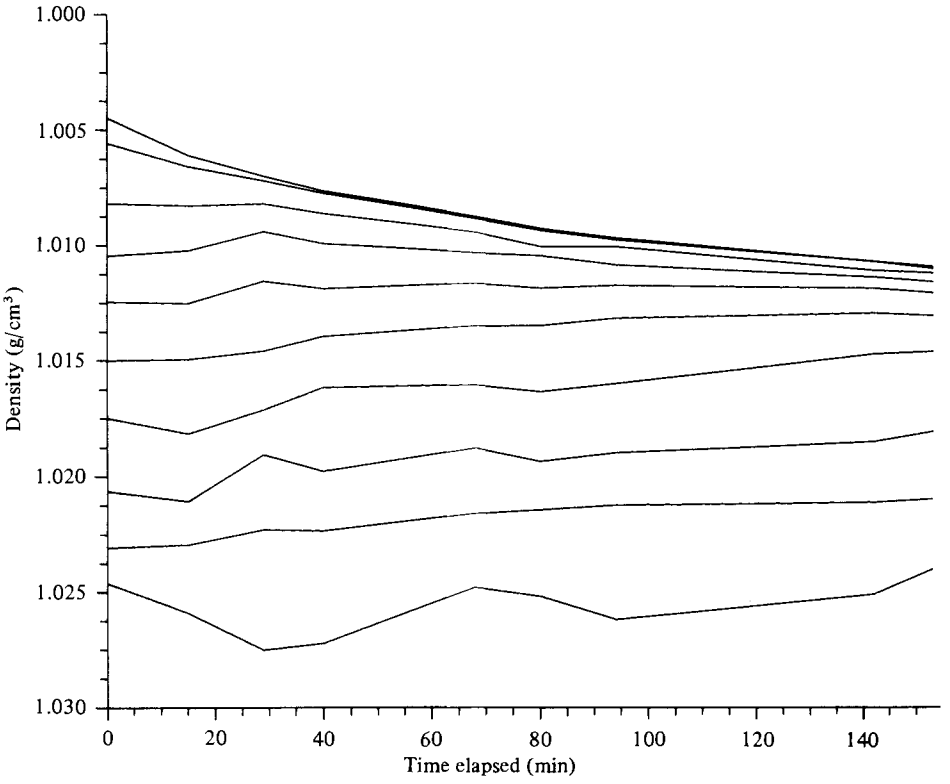

FIGURE 9. Density-profile decay for a constant-shear profile with $\partial\overline{U}/\partial z = 0.87\ \mathrm{s}^{-1}$.

The persistence of the initial density gradients is partly due to the fact that the supply tanks contain a large percentage of the total water volume. Only 10 % of the water available in any one layer is mixed before returning to the tanks. The cycle time for a parcel of water moving at maximum velocity, however, is only about 2 min, which implies that initially minimal mixing occurs in any one pass of the test section under high-stability conditions.

Frictional heating of the water causes an increase in tunnel temperature and could affect density profiles. The rate of temperature rise observed is about 1.4 °C/h but is found to be the same for each layer. Thus profiles are not altered by unequal heating of the various layers. However, temperature correction of the hot-film and salinity-probe instrumentation is necessary to account for the mean temperature drift.

Figures 7–10 illustrate that experiments studying the decay of grid-generated turbulence can be done under locally constant conditions if the probe sensors are placed in the inner core region of the flow and the density profile and temperature are recorded at every data station. The profile then is considered constant only for that station. By monitoring the density profile every time data is recorded, the evolution of the flow through a broad range of stability conditions can be studied in one continuous run of the channel.

The instrument platform is designed so that density profiles are easy to obtain and can be displayed directly on an (x, y)-recorder. The rate of change of the gradient can easily be monitored for any particular experiment while it is in progress.

Active control is required to maintain constant density conditions at the test-section inlet. Using mixing-rate data for a particular experimental setup as in figures 7 and

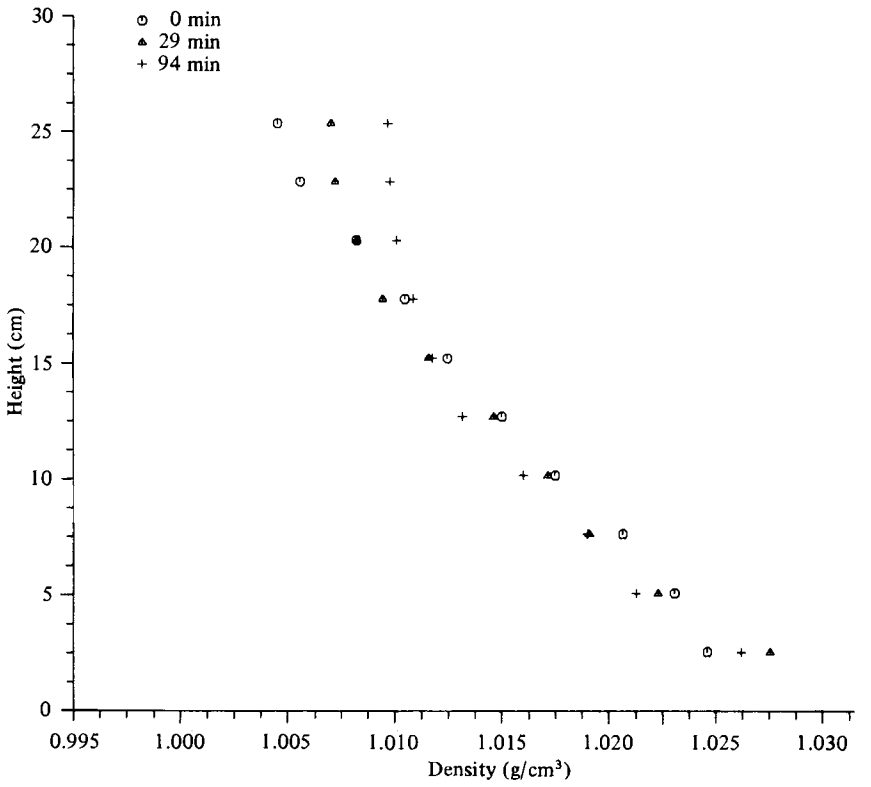

FIGURE 10. Density profiles at three times in a stratified experiment for a constant-shear profile with $\partial\overline{U}/\partial z = 0.87\ \mathrm{s}^{-1}$.

9 a scheme to predict amounts of fresh or saturated salt water to be added to each layer could be implemented in the future. In operation the density in each layer would be continuously monitored and fed to a microprocessor that determines the flow rate of fresh water or brine needed to maintain the correct density in that layer. Solenoid valves connected to large supply manifolds could be cycled by the microprocessor to produce the correct flow rates.

6. Water-channel operating parameters

The range of experiments possible in the stratified-flow water channel is illustrated by estimates of some important physical parameters achieved under various operating conditions. They are tabulated in table 1. In these estimates, it is useful to define two classes of operating conditions that bound the range of gradients used in the experiments. First, 'uniform' gradients of velocity or density refer to the existence of a constant gradient across the total ten-layer height of the channel test section. Second, we refer to 'discrete' velocity and density gradients when the change in velocity or density makes its total change over a vertical length corresponding to one layer thickness, about 2.54 cm. Other velocity and density profiles are entirely feasible, but the above will serve to characterize the realistic range of the important parameters achievable in the facility.

The mean speed U of all layers or of any individual layer ranges from 0 to about 30 cm/s. Use of the gravity-driven flow and control valves permits U to be exactly

$\frac{\partial\rho}{\partial z}$ (g/cm⁴)	N (s⁻¹)	f_N (Hz)	T_{BV} (s)	$\overline{U}$ (cm/s) 12.0	25.0	$\overline{U}$ (cm/s) 12.0	25.0	$\left\|\frac{\partial\overline{U}}{\partial z}\right\|$ (s⁻¹) 0.6	1.2
				Fr_m		$T_{BV_{100}}$		Ri_g	
-4×10^{-3}	1.93	0.31	3.3	3.26	6.8	4.8	2.3	10.3	2.6
-1.0×10^{-3}	0.98	0.16	6.4	6.43	13.4	2.5	1.2	2.7	0.7
-1.0×10^{-4}	0.31	0.05	20.3	20.3	42.3	0.78	0.38	0.27	0.07
-1.0×10^{-5}	0.10	0.016	62.8	63.0	132.2	0.25	0.12	0.03	0.007
0	0	0	∞	∞	∞	0	0	0	0
								$\left\|\frac{\partial\overline{U}}{\partial z}\right\|$ (s⁻¹) 6.0	12.0
-4×10^{-2}	6.06	0.96	1.04	1.04	2.2	15.3	7.3	1.02	0.26
-1×10^{-2}	3.10	0.50	2.02	2.03	4.23	7.9	3.8	0.27	0.07
-5×10^{-4}	0.70	0.11	8.98	9.0	18.75	1.8	0.85	0.01	0.003
-4×10^{-5}	0.20	0.032	31.7	31.5	65.6	0.5	0.24	0.001	0.0003
0	0	0	∞	∞	∞	0	0	0	0

TABLE 1. Stratified-water-tunnel operating parameters

zero or as close to zero as desired. This is not always the case in some facilities with pump-driven flows as the pumps do not operate well at slow speeds. For the grid mesh length $M = 1.905$ cm used for the present experiments the maximum grid Reynolds number $Re_m = Um/\nu$ is about 5700, and the maximum $x/m = 260$, where x is the longitudinal distance downstream from the grid. As noted in §5, $x/m = 100$ is the furthest station used for turbulent-decay studies owing to background turbulence levels. At $x/m = 100$ the sidewall boundary-layer thickness, assuming a turbulent boundary layer, is approximately 5 cm.

Experience with salt water has shown that it is best to keep the maximum density from exceeding 1.1 g/cm³ to reduce the problem of salt coming out of solution and collecting at various points in the system. This implies that normally the maximum $\Delta\rho$ that can be achieved is 0.1 g/cm³ and that the uniform density gradients will be in the range -0.004 g/cm⁴ $< \partial\rho/\partial z < 0.004$ g/cm⁴. The discrete density gradients will be in the range -0.04 g/cm⁴ $< \partial\rho/\partial z < 0.04$ g/cm⁴. All experiments that have been performed to date have utilized stable ($\partial\rho/\partial z < 0$) gradients.

With these density gradients, the Brunt–Väisälä frequency $N = (-g/\rho\,(\partial\rho/\partial z))^{\frac{1}{2}}$, which is the intrinsic vertical oscillation frequency of a parcel of fluid in the gradient field, ranges between $0 < N < 1.93$ s⁻¹ for the stable uniform gradient condition and $0 < N < 6.11$ s⁻¹ for the discrete gradient condition. The Brunt–Väisälä period $T_{BV} = 2\pi/N$, and the numbers of BV periods corresponding to 100 mesh lengths for various flow conditions are shown in table 1.

A global parameter useful in comparing various flow facilities is the overall Froude number Fr. It is a non-dimensional ratio comparing inertial forces to buoyancy forces, and is defined as

$$Fr = \left(\frac{U^2\rho}{g\Delta\rho L}\right)^{\frac{1}{2}},$$

where L is the length over which the maximum density difference $\Delta\rho$ occurs. U is the mean-flow velocity and g the gravitational acceleration. The values of Fr_m based on grid mesh size m attainable in the facility are listed in table 1.

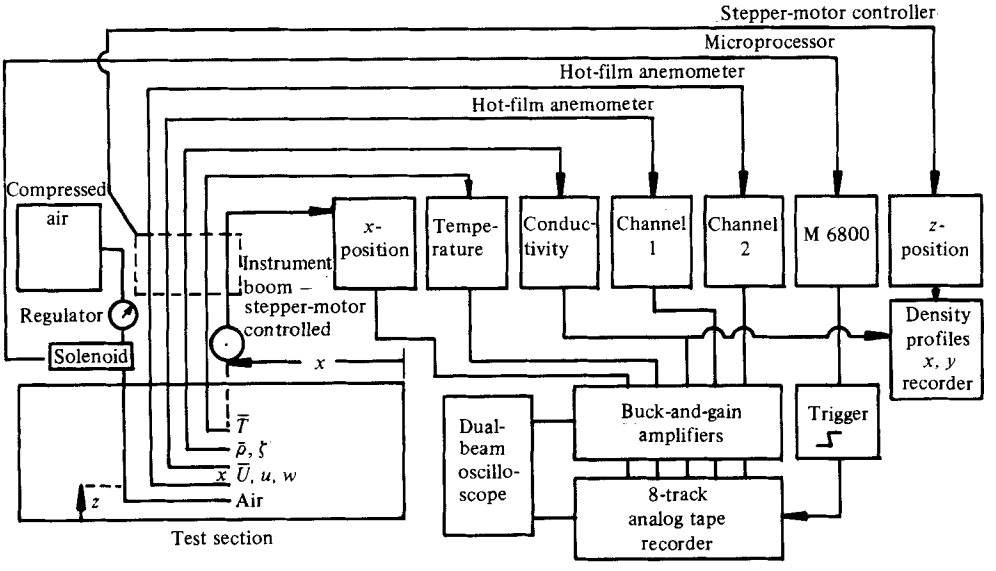

FIGURE 11. Instrumentation diagram – UCSD stratified water channel.

The gradient Richardson number Ri_g, defined as $Ri_g = N^2/(\partial\bar{U}/\partial z)^2$, is one of the most important parameters governing flow stability. For the uniform velocity gradient condition the shear ranges from $-1.2\ s^{-1} < \partial U/\partial z < 1.2\ s^{-1}$ and for the discrete velocity gradient conditions from $-12.0\ s^{-1} < \partial U/\partial z < 12.0\ s^{-1}$. Corresponding values of Ri_g obtainable in this facility are shown in table 1.

7. Instrumentation

Three probes are presently used for velocity and density measurements in the facility, a quartz-coated X-film for horizontal and vertical velocity measurements, a platinum resistance thermometer for mean-temperature measurements to correct the X-films, and a microscale conductivity probe for density measurements.

A block diagram outlining the mean features of the instrumentation system is shown in figure 11. Instruments are mounted in the test section on a movable carriage, which runs the entire length of the channel on tracks. Precision ball-bearing wheels are utilized to minimize vibration of the instruments.

Mounted within the carriage is a stepper motor-driven instrument boom designed so that vertical traverses can be made throughout the entire depth of the channel with a position resolution of 0.1 mm/step. The stepper motor-drive system includes a digital-to-analog convertor providing an analog position output. Rapid traversing of the boom at 250 steps/s allows for quick profiling of the channel any time during an experiment to obtain various vertical gradients.

The carriage has a fifth wheel, which also rides on the channel track and is coupled to a precision multiturn potentiometer, providing information on the horizontal position and velocity of the carriage.

The design of the instrumentation carriage has several advantages. Probes mounted on the boom can be moved quickly to any point in the vertical centreplane of the channel. Surveys of vertical profiles can be done quickly and repeated often, so monitoring of the mean gradients in the channel is possible throughout an experiment. The carriage can also be used to do direct calibrations of X-film probes.

The calibration of X-films within the test facility is desirable because the mounting geometry of the probe, on which the calibration constants are dependent, remains fixed. Prerun and postrun calibrations are possible with little effort and encompass temperature and density conditions present through an experiment.

Following the approach used by Koop (1976), the carriage is accelerated along the track using a weight and pulley arrangement. The instrument boom is yawed relative to the towing direction, thus exposing the X-film sensors to a continuous distribution of known velocity components. The carriage position and the two film voltages are digitized directly and the Interdata 7/16 minicomputer generates the calibration coefficients.

Operation of the hot-film instrumentation in this channel is subject to two serious problems. (i) Bubble formation on the sensor surfaces occur even when the hot films are operated as low as 10 °C above the ambient fluid temperature. Dissolved gases in the water tend to come out of solution on the heated films even before local boiling would occur (Pao 1973). Therefore the heat-transfer characteristics of the films change, resulting in calibration shifts. The resultant anemometer output voltage tends to drop, imparting a low-frequency drift to the data. (ii) The low film temperatures required to minimize the bubbling effect cause the X-films to be highly sensitive to temperature.

The use of hot films in this water channel is further complicated because of the mean-temperature increase of about 1.4 °C per hour due to frictional heating of the water. This temperature rise has drastic effects on the film's calibration. A temperature compensation scheme must be used in order to operate the hot films with any success at all.

The approach adopted consisted of monitoring the mean temperature throughout an experiment and using a modified King's law to correct the film response for temperature. Castaldini, Helland & Malvestuto (1980) have shown that the modified King's law

$$E_b^2 = A + B\left(\frac{U}{\rho}\right)^n (T_f - T_a) \tag{4}$$

describes the response of hot films in aqueous NaCl flows. Here E_b is the anemometer bridge voltage, U, ρ and T_a the velocity, density and ambient temperature of the fluid, T_f the film temperature, and A, B and n calibration constants. They show that the film response is only weakly sensitive to changes in density, so no attempts were made to correct for this change.

A calibration is performed both before and after each experiment at the lowest and highest temperatures encountered. From these calibrations A, B, n and T_f can be determined, and the data are then corrected at the time of analysis.

Figure 12 shows an uncorrected calibration of a hot film for two temperatures spanning a typical run. The data were fitted to the usual King's law for isothermal operation, i.e. $E_b^2 = A + BU^n$. It illustrates the dramatic effects temperature has on film response. Figure 13 shows the same calibration data plotted in corrected form using (4). Similar plots are generated for each film in the X-array.

Erratic calibrations were obtained for X-films that were not insulated adequately from the salt water by their quartz coating. Several films from one manufacturer could not be consistently calibrated and showed such conduction to the water. Resistances greater than about 10 MΩ between the ground plane in the channel and each film are necessary for consistent results.

The solution to the bubble-formation problem was handled by adaptation of a technique used by Grant, Stewart & Moilliet (1962) to clean film probes on towed

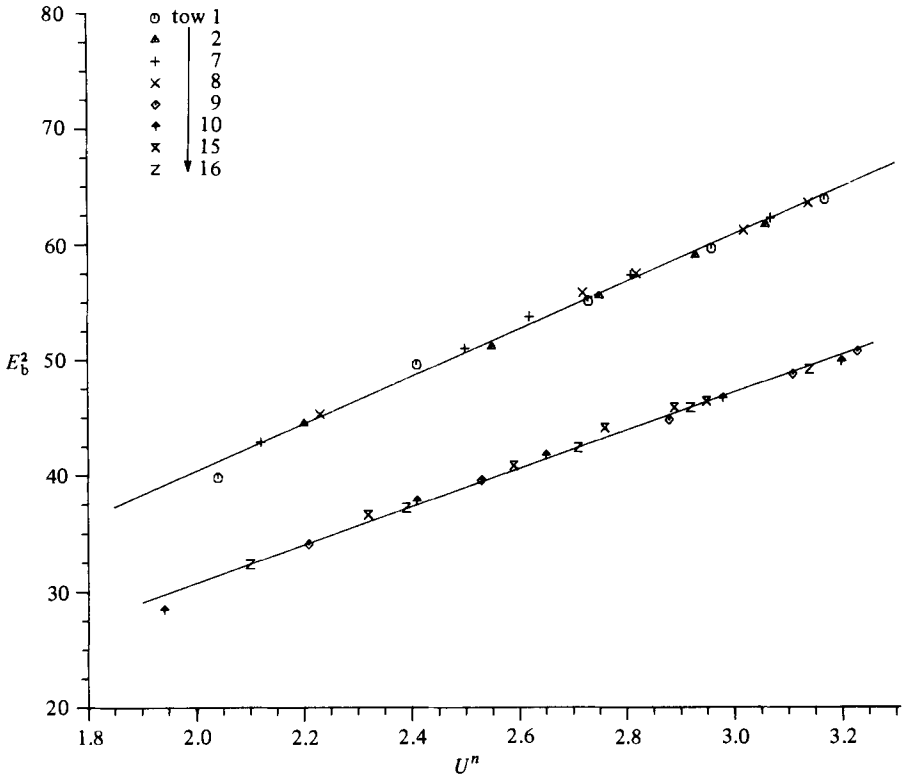

FIGURE 12. Hot-film calibration uncorrected for temperature using King's law for isothermal operation. Tows 1, 2, 7, 8 at 19.96 °C; tows 9, 10, 15, 16 at 22.40 °C; film temperature $T_f = 30.86$ °C.

bodies in the ocean. Periodically, the measurements were interrupted and a high-pressure stream of air was directed from a nozzle located below and behind the X-film array onto the sensors, thus sweeping away any bubbles attached to the films. In this manner large numbers of records could be acquired without the tremendous low-frequency drift that occurs when the probe is not washed periodically.

A microscale conductivity instrument (MSCI) developed by Head (1983) having both high resolution and good stability is used for density measurements. This instrument uses four electrodes to achieve stability, has a frequency bandwidth of 800 Hz, and a spatial bandwidth of 4 cycles/cm. The MSCI is calibrated by dipping its electrode into a few solutions of known concentration of sodium chloride solution. Mean temperature T and MSCI output voltage V_0 is recorded. The specific conductivity σ of the solution is calculated, and a least-squares fit of the form

$$V_0 = q\sigma + V_{\text{offset}} \tag{5}$$

is made. Calibration made before and after an experiment differ by less than 1 %. The MSCI gives observations of σ. The desired parameter, solution density, is calculated from σ and T (also measured).

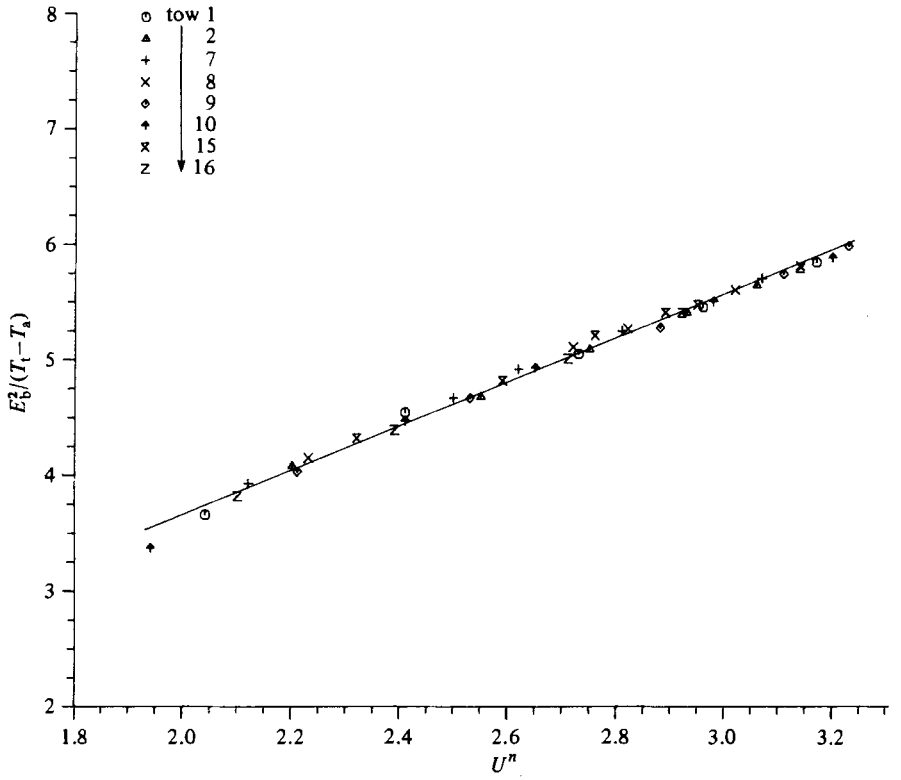

FIGURE 13. Hot film corrected for temperature using a modified King's law. Tows 1, 2, 7, 8 at 19.96 °C; tows 9, 10, 15, 16 at 22.40 °C; film temperature $T_f = 30.86$ °C.

8. Conclusions

A continuous-circulation stratified water channel containing 10 gravity-driven layers has been successfully developed. Each layer can be independently adjusted for velocities from 0 to 30 cm/s and densities from 1.0 to 1.1 g/cm^3 using salt brine as the stratification agent.

Inherent high turbulence levels caused by the ten mixing layers present at the test-section inlet can be reduced using a foam-and-screen management device placed at the inlet manifold. The inherent step structures of both the velocity and density profiles are also smoothed by the technique. Velocity can be held constant and continuity achieved in each layer such that given arbitrary velocity profiles can be maintained for any length of time.

Density profiles do change slowly in time depending on the initial stable stratification and velocity profile. The inner layers of the flow maintain a linear gradient throughout a stratified run. The slope slowly increases such that for many stratified turbulence experiments the gradient can be considered constant for short periods of time. Using this feature several stratified-flow experiments can be run with the same velocity profile by simply repeating measurements separated in time to ensure that successively weaker density gradients are generated at the test section inlet.

Internal heating of the system causes a temperature rise of approximately 1 °C per hour in the channel. This inherent contamination makes necessary the use of

temperature-correction techniques for hot-film anemometry and density measurements. Successful methods of compensation and calibration of the instrumentation are easily applied to correct these measurements.

This research was supported in part by the National Science Foundation under Grants CME78-25088 and OCE78-09060.

REFERENCES

CASTALDINI, M., HELLAND, K. N. & MALVESTUTO, V. 1980 Hot film anemometry in aqueous NaCl solutions. *Int. J. Heat Mass Transfer* **24**, 133.

DICKEY, T. D. & MELLOR, G. L. 1980 Decaying turbulence in neutral and stratified fluids. *J. Fluid Mech.* **99**, 13.

GIBSON, C. H. 1980 Fossil temperature, salinity, and vorticity in the ocean. In *Marine Turbulence* (ed. J. C. T. Nihoul), p. 221. Elsevier.

GIBSON, C. H. 1981 Buoyancy effects in turbulent mixing: sampling turbulence in the stratified ocean. *AIAA J.* **19**, 1394.

GRANT, H. L., STEWART, R. W. & MOILLIET, A. 1962 Turbulent spectra from a tidal channel. *J. Fluid Mech.* **12**, 241.

HEAD, M. J. 1983 The use of miniature four-electrode conductivity probes for high resolution measurement of turbulent density or temperature variations in salt-stratified water flows. Ph.D. thesis, University of California, San Diego.

KOOP, G. C. 1976 Instability and turbulence in a stratified shear layer. Ph.D. thesis, University of Southern California.

LANGE, R. E. 1974 Decay of turbulence in stratified water. Ph.D. thesis, University of California, San Diego.

LIN, J. T. & BINDER, G. J. 1967 Simulation of mountain in a wind tunnel. *College of Engng, Colorado State Univ. Int. Rep.* CER67-88 JTL-6JB24.

LIN, J. T. & VEENHUIZEN, S. D. 1974 Measurements of the decay of grid generated turbulence in a stably stratified fluid. *Bull. Am. Phys. Soc.* **19**, 1142.

MONTGOMERY, R. D. 1974 An experimental study of grid turbulence in a thermally-stratified flow. Ph.D. thesis, University of Michigan.

ODELL, G. M. & KOVASZNAY, L. G. 1971 A new type of water channel with density stratification. *J. Fluid Mech.* **50**, 335.

OSBORN, T. R. 1980 Estimates of the local rate of vertical diffusion from dissipation measurements. *J. Phys. Oceanogr.* **10**, 83.

PAO, Y. H. 1973 Measurements of internal waves and turbulence in two dimensional stratified shear flows. *Boundary Layer Met.* **5**, 177.

SCOTTI, R. S. 1969 An experimental study of a stratified shear layer. *Aero. Sci. Div., Univ. of California Int. Tech. Rep.* A5-69-1.

STILLINGER, D. C. 1981 An experimental study of the transition of grid turbulence to internal waves in a salt-stratified water channel. Ph.D. thesis, University of California, San Diego.

STILLINGER, D. C., HELLAND, K. N. & VAN ATTA, C. W. 1983 Experiments on the transition of homogeneous turbulence to internal waves in a stratified fluid. *J. Fluid Mech.* **131**, 91–122.

WEBSTER, C. A. G. 1964 An experimental study of turbulence in a density-stratified shear flow. *J. Fluid Mech.* **19**, 221.